Kovove Mater. 51 2013 111–115
DOI: 10.4149/km_2013_2_111

A new method to improve tribological properties of titanium by means of Al-Mg intermetallic matrix composite coatings

P. Liu[1]*, S. Li[2], Y. Zhang[1], H. Luo[1], Y. Huo[1]

[1]*School of Materials Science and Engineering, Shandong Jianzhu University, Jinan 250101, P. R. China*
[2]*Shandong Labor Vocational and Technical College, Jinan 250022, P. R. China*

Received 21 April 2012, received in revised form 29 September 2012, accepted 5 October 2012

Abstract

In this study, the Al/Mg powders were firstly used to improve the wear resistance of titanium by means of the laser cladding technique, which possesses a great potential in the field of surface modifications. The synthesis of the hard composite coating on pure Ti by laser cladding of the Al-Mg-B_4C or Al-Mg-B_4C-Fe pre-placed powders was investigated in detail. SEM results indicated that an Al-Mg intermetallic matrix composite coating with metallurgical joint to the substrate was formed. Compared with pure Ti, the improvement of the micro-hardness and wear resistance for such composite coating was observed.

K e y w o r d s: surface modifications, laser processing, composites, Al-Mg intermetallics

1. Introduction

Laser cladding is a useful surface modification technique, because of the following advantages: optimal bond properties, high process flexibility, rapid solidification and no requirement for post-process treatment. Use of laser clad composite coating is an effective way to improve the surface performance of titanium and its alloys [1, 2].

Mg alloys are the best and lightest metal materials which are widely used in high technology fields, such as automotive, electro- and aerospace industries [3, 4]. Fe-Al intermetallics are regarded as potential high--temperature structure materials for industrial application, with good properties of the wear, corrosion and oxidation resistance [5, 6]. Ti-Al intermetallics have been examined and developed for high temperature applications, which showed the high wear resistance, low density, high oxidation resistance and good mechanical behavior with temperature [7]. Laser cladding of the Al/Mg + B_4C pre-placed powders on pure Ti can form the TiC/TiB_2 reinforced composite coating, which increased the wear resistance of pure Ti. Through the experiment, it was found that with addition of proper Fe content, TiB_2 had more time to grow up, which strengthened the crystal boundary of the coatings, leading to the improvement of tribological properties.

In this study, the microstructures and tribological properties of the Al-Mg intermetallic matrix composite coatings are investigated in detail.

2. Experimental

Materials used in this experiment: the Ti samples, size of 10 mm × 10 mm × 10 mm, were polished with abrasive paper prior to the coating operation. The pre--placed powders of Al ($\geq$ 99.5 % purity, 50–150 μm), Mg ($\geq$ 99.5 % purity, 150–250 μm), B_4C ($\geq$ 99.5 % purity, 50–100 μm) and Fe ($\geq$ 98.5 %, 50–100 μm) were used for the laser cladding. The thickness of the pre-placed coating was 0.8 mm. The parameters of these three samples were the same during the cladding process. Cross-flow CO_2 laser with a beam diameter of 4 mm was employed to melt the surface of the samples. During the cladding process, argon gas at a pressure of 0.4 MPa was fed through a nozzle which was coaxial with the laser beam. The parameters and materials of the laser cladding process in experiment are shown in Table 1.

Parameters of these two samples were the same

*Corresponding author: tel.: +86 13256705460; fax: +86 0531 87918269; e-mail address: liupeng_qlzs@163.com

Table 1. The parameters and the materials of the laser cladding process in the experiment

Number	Substrate materials	Powders composition (wt.%)	Laser power (kW)	Scanning speed ($mm\,s^{-1}$)	Spot diameter (mm)
1	Ti	39Al-26Mg-35B_4C	0.7–0.95	2–7	4
2		33Al-22Mg-35B_4C-10Fe			

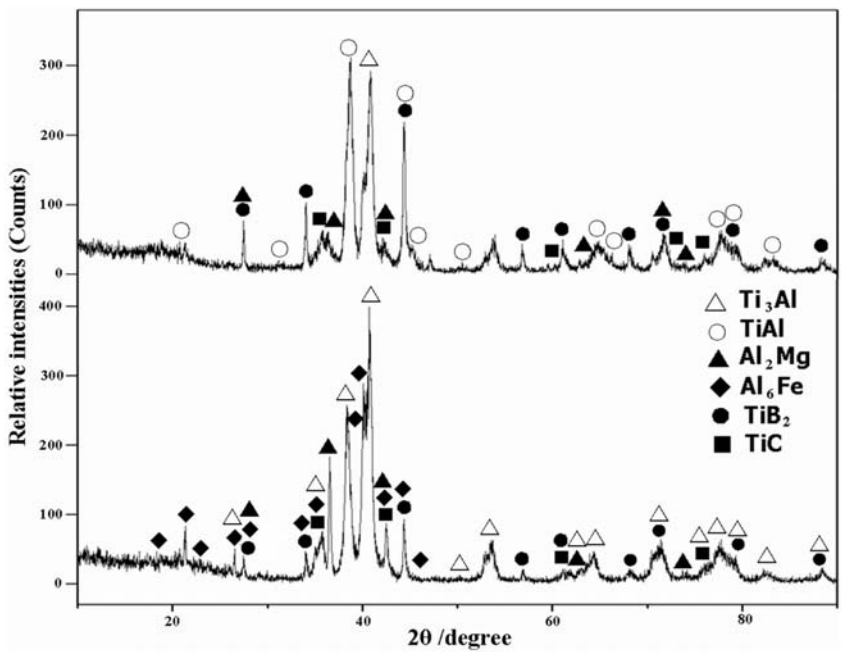

Fig. 1. X-ray diffraction diagram of the laser-cladded composite coating in samples 1 and 2.

during the cladding process. The wear volume loss was measured in 15 min interval. The wear properties of the laser-cladded coatings were tested by WMM-W1 disc wear tester. The rotational speed of the wear tester was 465 rpm. The linear velocity of the friction surface was $0.88\,m\,s^{-1}$. The microstructures of the composite coatings were identified with Hitachi transmission electron microscopy (TEM) (JEOL ARM 200F). SMX-1000/1000L X-ray diffractometer (XRD) was used to determine the phase constituent of the coatings. Microscope analysis was used to observe the microstructure characteristics of the coatings. The microstructural morphology of the composite coatings was analyzed by means of A LEO 1525 scanning electron microscope (SEM). HV-1000 micro-sclerometer was used to test the micro-hardness distribution.

3. Experimental results and analysis

3.1. XRD, SEM and EDS analysis

The XRD result of the coating in samples 1 and 2 is shown in Fig. 1. It was found that the coating in sample 1 consisted of Ti_3Al, TiAl, Al_2Mg, TiB_2 and TiC. In fact, due to the dilution effect, a part of Ti entered into the molten pool from the substrate. The XRD result indicated that Ti_3Al, TiAl, Al_2Mg, TiB_2 and TiC can be produced through the in situ metallurgical reactions during the laser cladding process. It was noted that with addition of Fe, the diffraction peak of Al_6Fe was present, and the Ti_3Al diffraction peak increased significantly. It was considered that the production of Al_6Fe consumed a large amount of Al in the molten metal, so Ti content was much higher than Al, which was favorable to the formation of Ti_3Al and the disappearance of TiAl. It was considered that the production of Ti_3Al consumed a large amount of Ti, which retarded the formations of TiB_2 and TiC to a certain extent.

The compact and fine microstructures of the composite coatings were obtained in samples 1 and 2 (Fig. 2). It was noted that the precipitates were dispersed uniformly in the matrix, which increased the micro-hardness and wear resistance of the coatings. Moreover, there was a metallurgical combination between the coating and the substrate in sample 1 or 2.

As shown in Fig. 3a, the TiC bulk-shape and TiB_2 stick-shape precipitates were produced in the bound-

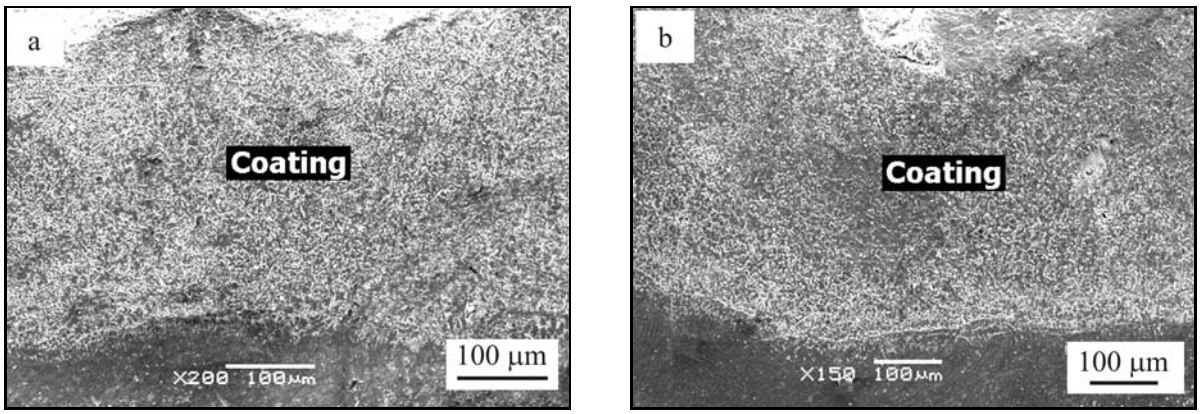

Fig. 2. SEM micrographs of the overview cross-section of the composite coatings in samples 1 (a) and 2 (b).

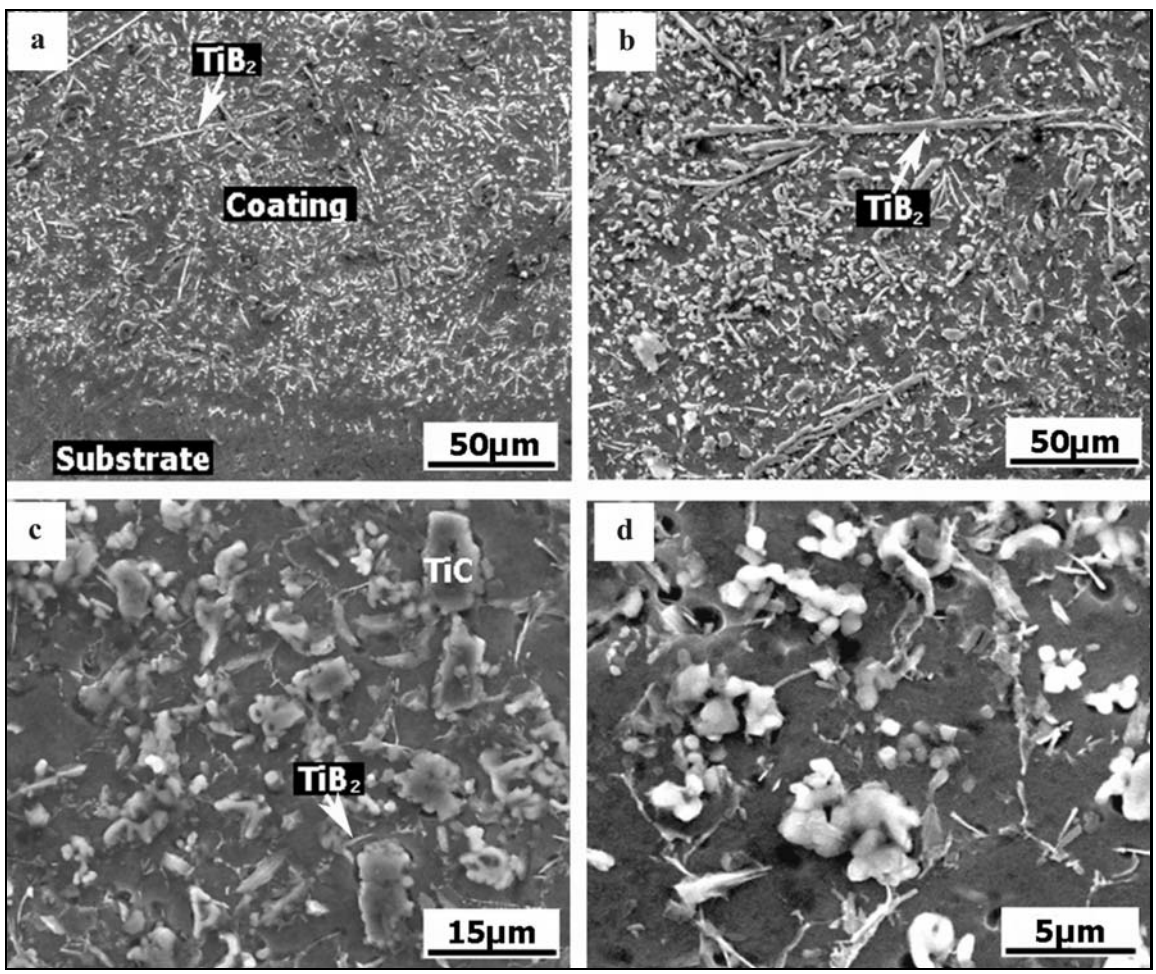

Fig. 3. SEM micrographs of the composite coatings: (a) bonding zone, and (b) clad zone in sample 2, (c) clad zone, and (d) the precipitates in sample 1.

ary zone of the sample 2. In fact, the TiB_2 precipitates were formed by the melting-dissolution – reprecipitation mechanism, i.e., TiB_2 melted and dissolved into the molten liquid. During the cooling process, TiB_2 nucleated and grew into the final reinforcement. In addition, most of the TiB_2 precipitates exhibited the fine acicular morphology due to the preferential growth of TiB_2 particle along the c axis ($\{0001\}$ direction) during the rapid cooling process. Due to the Gaussian distribution of the laser energy, the bottom of the molten pool absorbed less energy from the laser beam than the other locations, leading to the shorter

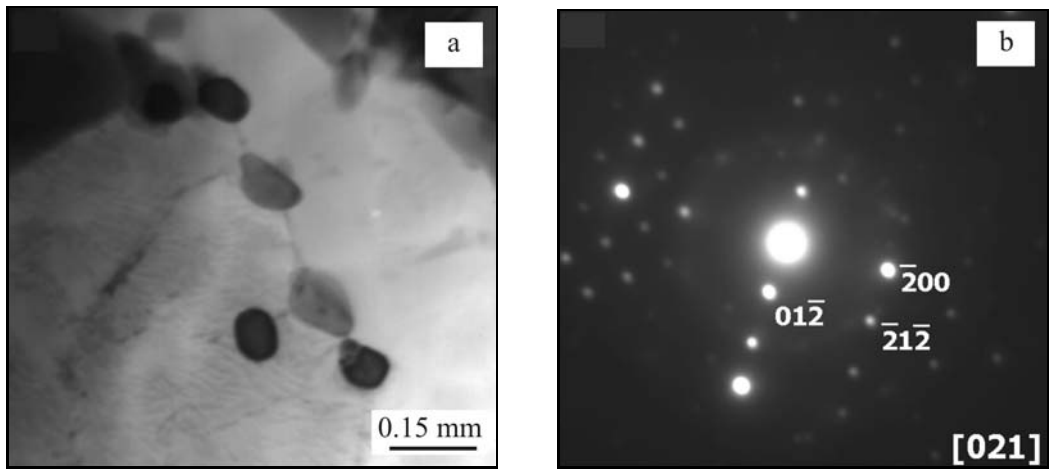

Fig. 4. Fine structure of Al_2Mg, TEM morphology (a), and electron diffraction pattern (b).

growth time of TiB_2 in this location. Thus, TiB_2 in the middle part of the molten pool obtained longer growth time than those of the bottom part (Fig. 3a,b). As shown in Fig. 3c, the TiB_2 precipitates in the coating of sample 1 were finer than those in sample 2. As mentioned previously, a large number of TiB_2 and TiC were produced in the coating of sample 1, which absorbed a large amount of energy from the laser beam, and it decreased the existing time of the molten pool. Thus, the growth time of TiB_2 was limited, leading to fine morphologies. As shown in Fig. 3d, the TiB_2 precipitates were produced at the grain boundaries of the matrix, and appeared as a small cluster [8]. Moreover, it was noted that the fine Al_2Mg block-shape precipitated in the coating, which showed a high micro-hardness [9]. The productions of Mg-Al intermetallics were found to improve the mechanical properties and enhance the corrosion resistance of the coating [9].

Further observing the clad zone, some bulk Al_2Mg intermetallic compounds were found near the crystal boundary of Ti_3Al (Fig. 4a), and the electron diffraction pattern is shown in Fig. 4b. The zone axis of Al_2Mg is B = [021]. Al_2Mg intermetallic compounds were dispersed in Ti_3Al/TiAl matrix, which is favorable to the improvement of wear resistance of the coating [10].

3.2. Micro-hardness and wear resistance

As shown in Fig. 5, the micro-hardness of the coating in sample 1 was in the range of 1270–1350 $HV_{0.2}$, which is approximately 6–7 times higher than that of the substrate (about 210 $HV_{0.2}$). The enhancement of the coating was mainly ascribed to its phase constituent and fine grain strengthening. Moreover, the micro-hardness distribution in the coating of sample 2 was in the range of 1300–1450 $HV_{0.2}$, which was slightly higher than that of the coating in sample 1. The higher micro-hardness was mainly ascribed to the

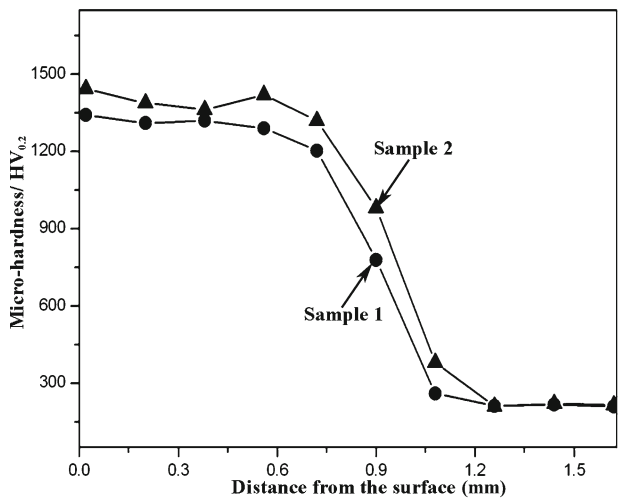

Fig. 5. Micro-hardness distribution in the composite coatings in samples 1 and 2.

action of high Ti_3Al and Al_6Fe content [11]. On the other hand, as mentioned previously, the TiB_2 precipitates had more time to grow up in the coating of sample 2, leading to the formations of the stick-shape precipitates, which strengthened the crystal boundary of the coating, favoring to increase the micro-hardness of the coating.

For the load of 54 N, the wear tester revealed that the wear volume loss of pure Ti substrate was 5–6 times higher than that of the coating in sample 2 (Fig. 6). However, the wear volume loss in sample 2 was only 2–3 times less than that of the substrate. It was speculated that the better wear resistance of the coating in sample 2 was ascribed to the higher micro-hardness. On the other hand, under the action of the pinning effect of the precipitates of the composite coating, the counterpart should overcome the number of these fine precipitates during the wear pro-

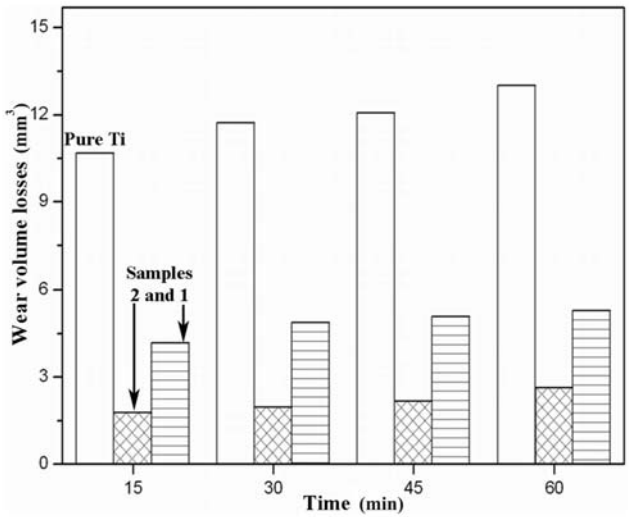

Fig. 6. Wear volume loss in Ti-6Al-4V alloy and in composite coatings in samples 1 and 2.

cess. The TiB_2 precipitates strengthened the crystal boundary, which was also beneficial in improving the wear properties of the coating. Thus, the coating in sample 2 showed the better wear resistance than that of sample 1.

4. Conclusions

TiC-TiB_2 reinforced composite coatings were fabricated on pure Ti by laser cladding of the Al/Mg + B_4C pre-placed powders. There was a metallurgical combination between such composite coating and the substrate. With addition of Fe, Al_6Fe was produced, which consumed a large amount of Al in molten pool, so Ti content was greatly higher than Al, which was favorable to the formation of Ti_3Al and the disappearance of TiAl. The production of Ti_3Al consumed a large amount of Ti, which retarded the formations of TiB_2-TiC in a certain extent. The micro-hardness distribution of the Al/Mg + B_4C pre-placed coating was in the range of 1270–1350 $HV_{0.2}$, which was approximately 6–7 times higher than that of the substrate (about 210 $HV_{0.2}$). With addition of 10 wt.% Fe, the micro-hardness of the coating was increased to 1300–1450 $HV_{0.2}$, and the wear volume loss was 5–6 times less than that of pure Ti.

Acknowledgements

This work was financially supported by the Science Foundation for Excellent Young Scientists of Shandong Province, China (grant no. BS2011CL027). Professor T. Zhai of University of Kentucky (USA) is gratefully acknowledged for the help in testing and for discussions about microstructures.

References

[1] Sun, R. L., Lei, Y. W., Niu, W.: Surf. Coat. Technol., *203*, 2009, p. 1395. doi:10.1016/j.surfcoat.2008.11.012
[2] Liu, P., Zhang, Y. B., Luo, H.: Surf. Eng., *28*, 2012, p. 531.
[3] Wang, S. R., Geng, H. R., Zhang, J. C., Wang, Y. Z.: Appl. Compos. Mater., *13*, 2006, p. 115. doi:10.1007/s10443-006-9015-x
[4] Li, Y. J., Liu, P., Wang, J., Ma, H. J.: Vacuum, *82*, 2008, p. 15. doi:10.1016/j.vacuum.2007.01.073
[5] Huang, W. Q., Li, Y. J., Wang, J., Shen, X. Q.: Kovove Mater., *48*, 2010, p. 227.
[6] Huang, W. Q., Li, Y. J., Wang, J.: Kovove Mater., *48*, 2010, p. 173.
[7] Li, J. N., Chen, C. Z., Squartini, T., He, Q. S.: Appl. Surf. Sci., *257*, 2010, p. 1550. doi:10.1016/j.apsusc.2010.08.094
[8] Li, J. N., Chen, C. Z., He, Q. S.: Mater. Chem. Phys., *133*, 2012, p. 741. doi:10.1016/j.matchemphys.2012.01.082
[9] Liu, P., Li, Y. J., Geng, H. R., Wang, J.: Mater. Lett., *59*, 2005, p. 2001. doi:10.1016/j.matlet.2005.02.038
[10] Liu, P., Li, Y. J., Geng, H. R., Wang, J.: Mater. Lett., *61*, 2007, p. 1288. doi:10.1016/j.matlet.2006.07.010
[11] Wang, S. R., Wang, Y., Li, C. C., Chi, Q., Fei, Z. Y.: Appl. Compos. Mater., *14*, 2007, p. 129. doi:10.1007/s10443-007-9036-0